A Modified Near-Field Gaussian Plume Inversion Method Using Multi-sUAS for Emission Quantification

Derek Hollenbeck[1,*] Demitrius Zulevic[1,2] and YangQuan Chen[1]

***Abstract*— This work introduces a modified near-field Gaussian plume inversion method (mod-NGI), for emission quantification from a point source using downwind vertical plane measurements. The original NGI method aims to solve the inverse problem by estimating model parameters using measured data and a partial parameter least squares fitting. Given noisy measurements, this can lead to ill-posed conditions, poor performance, and sensitivities to initial conditions. The mod-NGI method combines preconditioned maximum likelihood parameter estimation with full parameter least squares optimization. The single sensor performance of mod-NGI method is explored with static and dynamic ground truth functions for fixed path (lawn mower and spiral) and adaptive path (extremum seeking control) planning strategies including a comparison with experimental NGI results. A high level multi-sUAS control strategy is developed for continuous parameter estimation using centroidal Voronoi tesselations and mod-NGI.**

I. INTRODUCTION

Emission quantification is important in many industries, such as with oil & gas, landfills, transportation, dairies, and more. The types of emissions seen in these applications can vary from stationary point/area sources, mobile point sources, or some combination thereof. Additionally, some sources are even intermittent, such as with automatic pressure relief valves in oil and gas systems. In the literature, there are several methods to quantify emissions of this sort. In [1], advanced methane quantification techniques are reviewed and broadly categorized as either simulation-based, optimization-based, mass balance based, image-based, or correlation-based. For this paper we will focus on a continuous point source Gaussian (PSG) optimization-based approach, namely, the Near-Field Gaussian Plume Inversion (NGI) [2]. The NGI method is a sUAS-based method first introduced in [2] and was devised to fit a PSG to a methane plume in near-field conditions (10-100 m range). This optimization method typically consist of spatially sampling down wind transects of a methane plume using a sUAS and attempting to fit the PSG model to the observed data. Other PSG methods use stationary (conditionally sampled PSG method [3]) or vehicle based measurements (recursive Bayesian PSG method [4], [5]). The NGI method was experimentally tested in [2], which resulted in upward methane source flux biases due to the manual sampling method used. This was further tested in [6] where these biases were corrected for through using more unbiased flight sampling paths (pre-programmed waypoints and lateral transects in a course-lock mode). Though the NGI method was relatively close to the true emission results in some of the surveys, the upper and lower uncertainty bounds calculated did encapsulate the true source flux values. The NGI method was further deployed in [7] at a gas extraction site in the UK where methane was detected and quantified from known cold venting from exploratory hydraulic fracturing.

One of the major fallbacks of this method is the tuning of the vertical scale factor, which requires several optimization runs to establish an overall emission estimate. This extra computation can make online implementation more difficult. In this work we:

1) establish a modified NGI method, based on the method proposed in [2], to improve computation and noise robustness.
2) simulate the performance of the mod-NGI method in static and dynamic plume settings.
3) introduce a multi-sUAS strategy, namely CVT-mod-NGI, to quantify emissions from dynamic plumes.

The paper is organized as follows: section II reviews the original NGI method; section III introduces the modified NGI method; section IV gives some simulation examples and results; and section V gives concluding remarks.

54 pt
0.75 in
19.1 mm

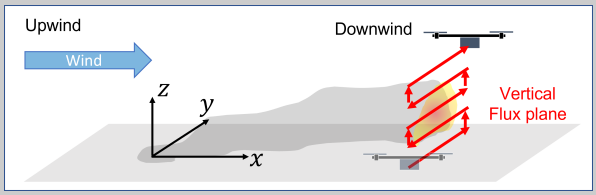

Fig. 1: A typical mass balance based flight path to quantify emission flux.

II. NEAR-FIELD GAUSSIAN PLUME INVERSE

The NGI method is an optimization method that seeks to solve an inverse problem by fitting a PSG model parameters, in terms of modeled methane flux q_{mo} found in (1), to a set of methane flux observations q_{me}. This is typically done by collecting flux plane observations upwind and downwind of the plume a distance x from the source (see Fig. 1). There are five unknown terms in (1): the methane source rate Q, the lateral and vertical plume centers μ_y & μ_z, and the lateral and vertical mixing terms σ_y & σ_z. For the NGI method, it is assumed that the vertical plume center is a known source height,

$$q_{mo} = \mathscr{M}(X,\theta) = QD_y(x,y;\sigma_y,\mu_y)D_z(x,z;\sigma_z,\mu_z), \qquad (1)$$

*Correspondence dhollenbeck@ucmerced.edu
[1]Department of Mechanical Engineering, University of California, Merced, 5200 N. Lake Rd, Merced, CA, 95343 USA.
[2]Physics Department, University of California, Merced, 5200 N. Lake Rd, Merced, CA, 95343 USA.

$$D_y(x,y;\sigma_y,\mu_y) = \frac{1}{\sqrt{2\pi}\sigma_y(x)} \exp\left(\frac{-(y-\mu_y)^2}{2\sigma_y(x)^2}\right), \quad (2)$$

$$D_z(x,z;\sigma_z,\mu_z) = \frac{\exp\left(\frac{-(z-\mu_z)^2}{2\sigma_z(x)^2}\right) + \exp\left(\frac{-(z+\mu_z)^2}{2\sigma_z(x)^2}\right)}{\sqrt{2\pi}\sigma_z(x)}, \quad (3)$$

where the i-th position vector is $X_i = [x,y,z]^T$, and the parameter vector is $\theta = [Q, \sigma_y, \sigma_z, \mu_y, \mu_z]^T$. It can be further assumed that $\sigma_y(x)$ and $\sigma_z(x)$ increase linearly with x under near-field conditions with variations in x less than 40 m. This is represented as $\sigma_y(x) = \tau_y x$ and $\sigma_z(x) = \tau_z x$. The experimentally measured flux is given as the difference between the raw methane ratio and the background methane ratio,

$$q_{me} = ([CH_4] - [CH_4]_0)U(z)\frac{PM}{TR}, \quad (4)$$

where $U(z)$ is the height dependent wind measurement, P is the atmospheric pressure, T is the temperature, and R is the gas constant. To avoid solving for five unknown parameters iteratively, the y-component ($q_{me,y}$) is solved for in (5),

$$q_{me,y} = q_{me}\frac{\tau_z x\sqrt{2\pi}}{\left(\exp\left(\frac{-(z-\mu_z)^2}{2(\tau_z x)^2}\right) + \exp\left(\frac{-(z+\mu_z)^2}{2(\tau_z x)^2}\right)\right)}. \quad (5)$$

Then using (5), μ_y and τ_y can be solved for with (6) and (7),

$$\mu_y = \frac{\sum_j (q_{me,yj} y_j)}{\sum_j (q_{me,yj})}, \quad (6)$$

$$\tau_y = \sqrt{\frac{\sum_j \left(q_{me,yj}\left(\frac{y_j-\mu_y}{x_j}\right)^2\right)}{\sum_j (q_{me,yj})}}. \quad (7)$$

It should be noted that (5), (6), and (7) require 'good spatial sampling' in the z-direction for estimating τ_z and Q [2]. Solving (5)-(7) simultaneously before optimizing allows for (1) to be constrained from the original five unknown parameters to only two unknown parameters (τ_z and Q). The original NGI method calls for τ_z and Q to be solved for through a least squares fitting function in MATLAB, known as *lsqcurvefit*. This function aims to solve a least squares cost function parameterized by Q and τ_z,

$$[\hat{Q}, \hat{\tau}_z] = \min_{Q,\tau_z} J(X;\phi), \quad J(X;\phi) = \sum_{i=1}^{N} (\mathscr{M}(X_i;\phi) - q_{me}^i)^2, \quad (8)$$

where $\phi = [Q, \tau_y, \tau_z, \mu_y, \mu_z]^T$. When optimizing, Q and τ_z are both bounded to a specified range (upper and lower bounds). It follows that the results are sensitive to the choice of $\tau_{z,max}$ (upper bound of τ_z) and to get a good estimate of Q, it is recommended by [2], that $\tau_{z,max}$ is incrementally increased until τ_z stabilizes - subsequently stabilizing Q. It is taken that $\tau_{z,max}$ is converged once it has reached within 2% of its previous iteration. This can be both tedious and vulnerable to inaccuracies due to the assumption that τ_z levels off with increasing $\tau_{z,max}$. Depending on where τ_z is initialized for the regressions, the final τ_z can settle in one of many local minima. The NGI method is not only sensitive to where the parameters are initialized, but also sensitive to the amount of noise.

For plume morphology, the NGI method assumes that the time averaged plume is Gaussian. Measurements of this time-averaged plume are considered to be unbiased. The plume is modeled to not be capped in the z-direction via an atmospheric temperature inversion and to be emitted from a point source. Due to the point source assumption, this model does not generalize well to area sources. In fact, it assumes that the model, $\mathscr{M}(X;\phi) = f(X;\phi) + \varepsilon$, where $\varepsilon \sim \mathscr{N}(0,\sigma_\varepsilon)$ is a normally distributed white noise and $f(\cdot)$ is the ground truth function (generally not known).

III. Modified Near-field Gaussian Plume Inverse

When noise is present in the data, the NGI method starts to becomes sensitive to initial conditions. The first question we can ask is, what is the best way to initialize the parameters? The second question is, can we further improve the optimization? To answer the first question let us consider a probability likelihood function that is represented by,

$$P(q|\theta) = D_y(x,y;\sigma_y,\mu_y)D_z(x,z;\sigma_z,\mu_z). \quad (9)$$

Consider that experimental measurements do not give access to the above likelihood function but can rather give an estimate of it and let's assume an initial source rate estimate $\hat{Q}$ such that,

$$\hat{P}(q_{me}|\hat{\theta}) \approx \frac{Q}{\hat{Q}} D_y(x,y;\hat{\sigma}_y,\hat{\mu}_y)D_z(x,z;\hat{\sigma}_z,\hat{\mu}_z). \quad (10)$$

The likelihood of observing the entire dataset then becomes,

$$\hat{P}(D|\hat{\theta}) = \Pi_{i=1}^{N} \hat{P}(q_{me}^i|\hat{\theta}). \quad (11)$$

Given that analytically solving for an optimizer using (3) can be complex, we make the assumption that the plume is far from the ground only for the parameter initialization steps. This allows for the approximation of (3) by,

$$D_z(x,z;\tau,\mu) \approx \frac{1}{\sqrt{2\pi}\sigma_z(x)} \exp\left(\frac{-(z-\mu_z)^2}{2\sigma_z(x)^2}\right). \quad (12)$$

Solving for the maximum log likelihood estimate (MLE) yields,

$$\hat{\tau}_y = \sqrt{\frac{1}{Nx^2}\sum_{i=1}^{N}(y_i-\mu_y)^2}, \quad \hat{\tau}_z = \sqrt{\frac{1}{Nx^2}\sum_{i=1}^{N}(z_i-\mu_z)^2}. \quad (13)$$

It can be readily apparent that the MLE is the definition of the standard deviation conditioned only on the spatial coordinates. To make this MLE conditioned on the flux measurements one can substitute for the weighted standard deviation. For example, the horizontal scale factor is given by,

$$\hat{\tau}_y = \sqrt{\frac{N}{(N-1)x^2}\frac{\sum_{i=1}^{N} q_{me}^i (y_i-\mu_y)^2}{\sum_{i=1}^{N} q_{me}^i}}. \quad (14)$$

In order to estimate τ_y and τ_z, the plume centers need to be computed. This is done using the measured flux as weights, and computing the center of mass,

$$\hat{\mu}_y = \frac{\sum_{i=1}^{N} q_{me}^i y_i}{\sum_{i=1}^{N} q_{me}^i}, \quad \hat{\mu}_z = \frac{\sum_{i=1}^{N} q_{me}^i z_i}{\sum_{i=1}^{N} q_{me}^i}. \quad (15)$$

Alternatively, the plume widths can be estimated directly without knowledge of plume location,

$$\hat{\sigma}_y = \sqrt{\frac{N}{(N-1)} \frac{\sum_{i=1}^{N} q_{me}^i (y_i - \mu_y)^2}{\sum_{i=1}^{N} q_{me}^i}}, \tag{16}$$

and similarly for σ_z. Once the dispersion and plume center parameters are estimated and a initial estimate of the source rate is established for $\hat{Q}$, the optimization of parameters θ can be undertaken, such that,

$$\hat{\theta} = \min_{\theta} J(X,\theta), \quad J(X,\theta) = \frac{1}{N}\sum_{i=1}^{N} (\mathscr{M}(X_i,\theta) - q_{me}^i)^2 \tag{17}$$

This optimization was carried out using the MATLAB *fminsearchbnd* function [8]. The complete mod-NGI approach is summarized in algorithm 1.

Algorithm 1: mod-NGI Method

Require:
Initial set of N flux observations $\{X, q_{me}\}_1^N$ inside the domain Ω_s;

Ensure:
Plume is sufficiently sampled inside Ω_s;

1: Compute maximum likelihood estimates of parameters $\hat{\mu}_y, \hat{\mu}_y, \hat{\tau}_y, \hat{\tau}_z \in \Omega_s$ using (14)-(15);
2: Initialize $\hat{Q}$ based on observations in $q_{me}^i \in \Omega_s$, (note: $Q \propto q_{me,max}$);
3: Perform cost function optimization given in (17) initialized with previously computed parameters.

IV. SIMULATION STUDIES

To illustrate the usefulness of the proposed method, a series of simulations are conducted comparing the NGI method and the mod-NGI method. It is assumed that the domain of interest contains the plume and the task is solely for quantification. It is also assumed that from the surface to 2 m is not accessible by the sUAS for safety reasons (see Fig. 2). Furthermore, let's consider that the sUAS is controllable at a high level and spatial position can be represented with single or double integrator dynamics.

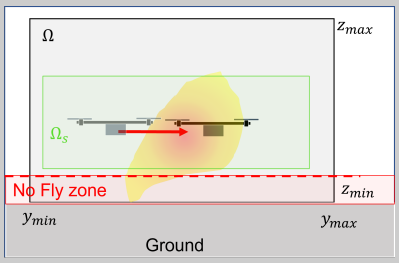

Fig. 2: The simulation sample domain.

There are two general types of path planning approaches explored here: simple fixed path planning (no vehicle dynamics), and adaptive path planning (single integrator dynamics). In the fixed path planning approaches, a lawnmower pattern (also referred to as raster scanning), and an Archimedes spiral was explored. For the adaptive path planning we look at extremum seeking control (ESC) and centroidal Voronoi tesselations (CVT) (see Fig. 3).

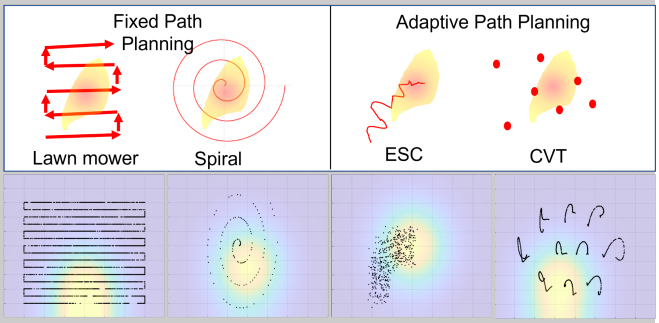

Fig. 3: This image illustrates the different path planning strategies to sample the plume.

A. Fixed Path Planning

1) Path Planning: To test the fixed path planning strategies a series of simulations were conducted, varying sample time, spacing between transects (or spirals) and the plume width (σ). It was observed that sample time and sample spacing (between transects) played an important role in reducing the variability of the estimations. For instance, as the sample time increased (i.e. more sparse), the performance (accuracy and precision of the θ estimates) degraded. Likewise, the sample spacing reflected the ability to capture the center of the plume, often leading to poor performance. The width of the plume, in conjunction with sample time, reflected the ability to even detect the plume. Thus, the performance given different plume widths, σ, was explored for lawnmower and spiral paths (see Fig. 4). Conversely, it can be observed that larger plume widths will lead to better estimations and less of a dependence on which path planning approach to choose. For fugitive and small emissions this is not often the case, since at larger plume widths (further distances downwind) the concentration becomes quite small and perhaps even unmeasurable.

Given a dynamic plume setting, where the plume location has an oscillation e.g. meandering wind that can infringe on the measurement process. To test the effectiveness, the amplitude of the plume meander is increased from 0 m (no meander) to 10 m for several frequencies given the same lawnmower flight path (1m transect spacing, 2 Hz sampling rate, 1m/s horizontal velocity and 10% relative noise). The results are shown in Fig. 5, where in some cases the source rate is not as affected and in other cases the source rate is under- and even over-estimated.

2) Comparison with experimental flight data: The mod-NGI method was compared with the results in [6] using their processed survey data. There were two DJI Spreading Wings S1000+ octocopter sUAS. The first was equipped with a perfluoroalkoxy tubing that tethers a local inlet on the UAV to a ABB Micro-portable Greenhouse Gas Analyzer (MGGA) on the ground. It was also equipped with a wind sensor.

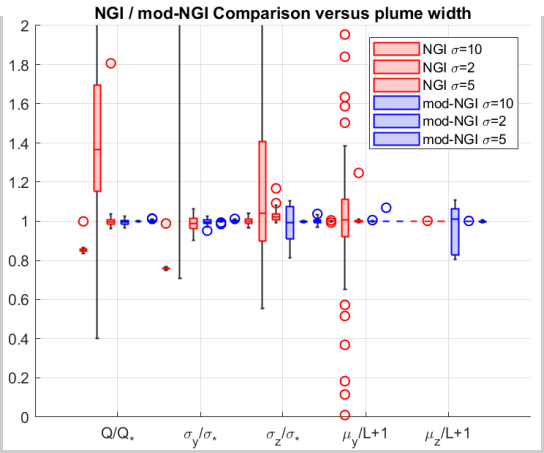

(a) Lawnmower with static plume.

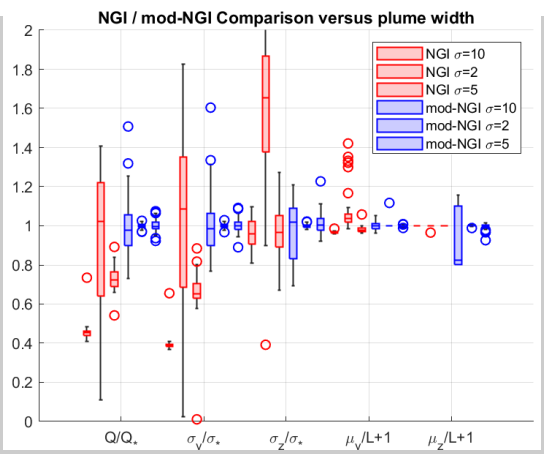

(b) Spiral with static plume

Fig. 4: In these boxplots, the estimation performance results for static plumes different plume widths are explored for (a) lawn mower & (b) spiral paths

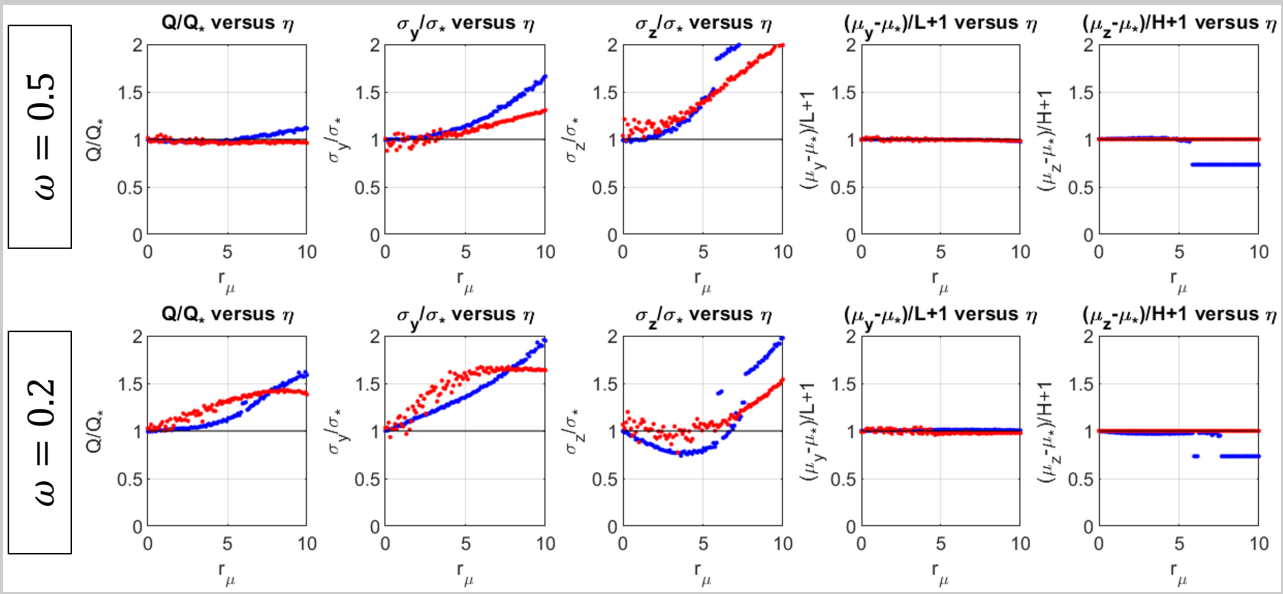

Fig. 5: In these sets of plots, the performance of the NGI (red) and the mod-NGI (blue) at different amplitudes of meandering are shown and the different frequency responses of the algorithms are shown in each row. It can be observed that both algorithms do not perform well given dynamic (e.g. meandering) conditions. The most variability can be seen in the plume width estimates.

The second was equipped with a lighter prototype MGGA (pMGGA). A two-dimensional stationary sonic anemometer was deployed near the boundary of the site for all surveys. The total data consisted of 22 flight surveys (7 for the first, and 15 for the second sUAS) was used to compare NGI and mod-NGI results (see Fig. 7). Though the mod-NGI method did not 'outperform' NGI, the results were still comparable.

B. Adaptive Path Planning

1) Single-sUAS Extremum Seeking Control (ESC): In nonlinear control theory, adaptive control is a very desirable topic, particularly if the model of the system is unknown or not accessible. Here we consider a model-free strategy called extremum seeking control (ESC), which aims to optimize a set of parameters using a perturbation signal and filtering. One of the first stability analysis works on ESC came from [9]. The ESC has been used to solve many problems, such as electric railway [10], maximum power point tracking [11], and plasma impedence matching [12]. The principle of ESC relies on the minimization of a cost function given some dynamical system. Here we treat the cost function as the concentration of the plume and seek to find the center (see Fig. 3). Given several values around the center of the plume, a reasonable estimate of the source could be made. However, the slope of the measurement field may not be smooth. This may lead to slow convergence times and trapping in local minima. It can be observed in Fig. 6d that given a dynamic

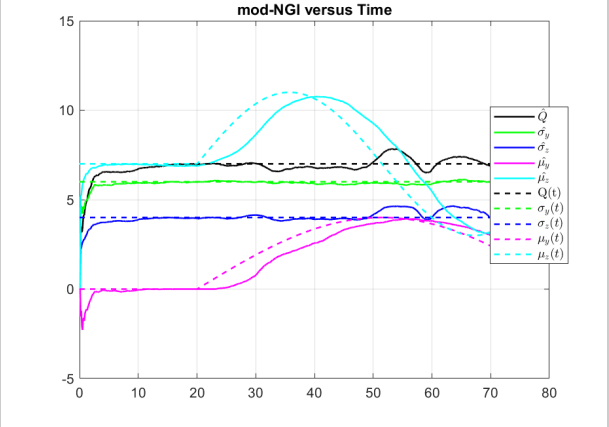

(a) CVT with $\omega = 0.1$ and 10 s window.

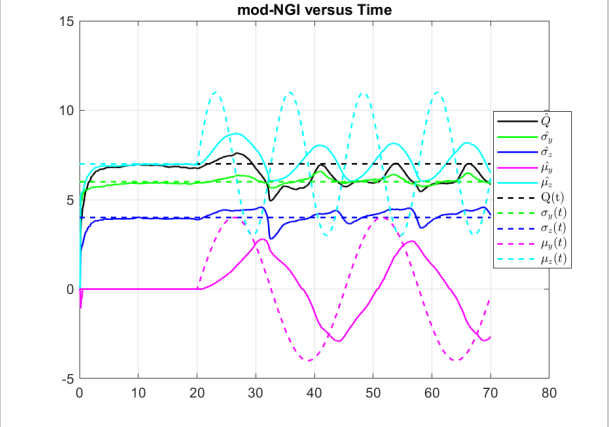

(b) CVT with $\omega = 0.5$ and 10 s window.

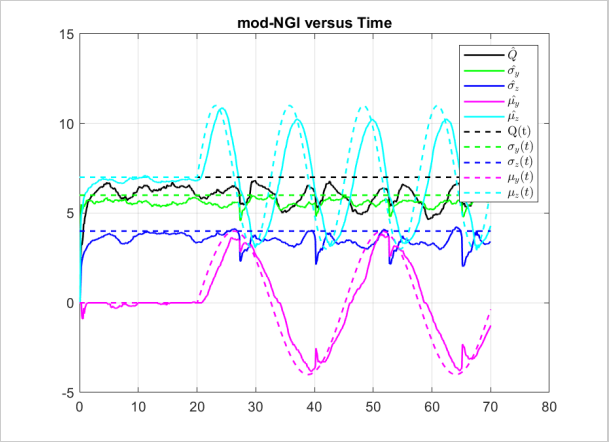

(c) CVT with $\omega = 0.5$ and 2 s window.

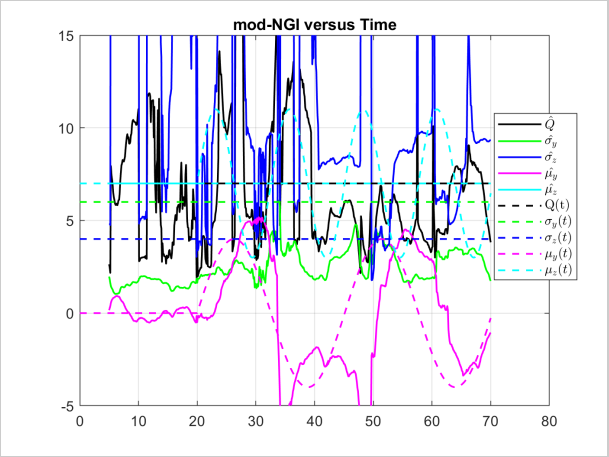

(d) ESC with $\omega = 0.5$ and 5 s window.

Fig. 6: Given a moving source these six plots show the effect of the multi-UAS CVT-mod-NGI and single ESC-mod-NGI based algorithms. It can be observed in plots (a)-(b) that as the movement frequency of the source increases the ability of the CVT-mod-NGI algorithm to estimate and track the source diminishes. This behavior is much like the response of a time series signal given a low pass filter. Conversely, as the window of points used to compute the mod-NGI approach is reduced, much like we would expect, the ability to track and estimate the parameters increases. Although the performance in (c) is improved, the estimations become more noisy, and thus there is a trade-off between tracking performance and stable estimations. To illustrate why multi-sUAS systems may be better, an ESC-mod-NGI algorithm is shown in (d), where the ability to estimate parameters is not as robust to meandering and exhibits more difficulty with hyperparameter tuning.

plume and slow convergence, mod-NGI estimations perform poorly with ESC given the frequency of meandering.

2) Multi-sUAS CVT: Taking into consideration all of the simulations thus far, they all utilize a single mobile sensor for estimation of the parameters. In this section we further explore adaptive path planning by introducing multi-sUAS coverage control strategy, namely, the centroidal Voronoi tesselations (CVT). The CVT strategy is brought into the mod-NGI approach to improve the robustness given a dynamic source (as seen in the previous sections). The CVT strategy looks to optimize the following cost function,

$$J(X) = \sum_{i=1}^{N} \int_{\mathcal{V}_i} \rho(\xi) |\xi - X_i|^2 d\xi, \text{ for } \xi \in \Omega. \tag{18}$$

Given the local positions of the sensors $X = (X_1, X_2, ...X_N)$, a domain of interest Ω can be divided into N polytopes $\mathcal{V} = (\mathcal{V}_1, \mathcal{V}_2, ...\mathcal{V}_N)$. The polytopes are determined using centroidal Voronoi tesselations [13]. The centroids, c_i, are computed using the density function $\rho(\xi)$ and positions are updated with Llyods algorithm [14]–[16], $\dot{X}_i = -k(X_i - c_i)$, where k is a proportional gain to be tuned. In this work we substitute the density function for, $\rho(X) = q_{mo}(X, \Theta)$. Here, $\Theta = [\hat{Q}, \sigma_y^c, \sigma_z^c, \mu_y^c, \mu_z^c]^T$, and the control parameters are related to the mod-NGI parameter estimations by,

$$\sigma^c = (1 + A_\sigma \sin(\omega_\sigma t))\hat{\sigma}, \tag{19}$$

$$\mu_y^c = A_\mu \cos(\omega_\mu t) + \hat{\mu}_y, \quad \mu_z^c = A_\mu \sin(\omega_\mu t) + \hat{\mu}_z. \tag{20}$$

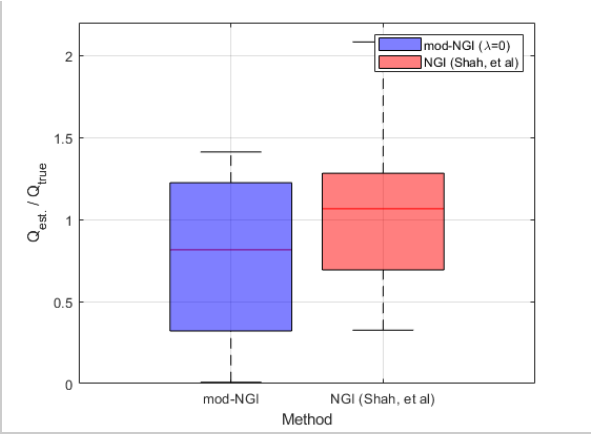

Fig. 7: Comparisons between the results from Shah et al.'s NGI, our NGI, the mod-NGI, and the true controlled release flux using the controlled release survey data from [6].

The results of this approach are shown in Fig. 6 given $A_\mu = \omega_\mu = 1$ and $A_\sigma = \omega_\sigma = 0.5$. The control parameters are time varying to introduce a persistent excitation signal into the sampling for improving exploration and parameter estimation convergence.

V. CONCLUSIONS

In this work we introduced the mod-NGI method for estimating emissions from mobile sensing data. The mod-NGI performance is compared with NGI in static and dynamic plume settings. The methods utilize fixed (lawnmower and spiral) and adaptive (ESC and CVT) path planning based measurements. For single mobile sensor approaches, the proposed method shows improved estimation accuracy and precision given static plume settings, however, when exposed to a dynamic plumes the performance particularly degrades in the source rate, and plume width estimations in both approaches. Regularization based optimization was also explored and offered little improvements in certain instances and degradation in others. The mod-NGI method seen comparable estimation results to previously published NGI data using controlled release survey data. Lastly, the results of the multi-sUAS adaptive path planning approach, CVT-mod-NGI, show good tracking and estimation performance. Furthermore, the use of multi-sensor strategies in simulation, outperform single sensor ones given a dynamic plume. This provides some motivation to utilize multi-sensor strategies in physical experimentation. Future work will look utilizing MOABS/DT [17] simulation (based on the ARPA-E METEC facility) to test the short time-scale behavior of the mod-NGI and CVT-mod-NGI methods. Additionally, comparison against controlled release mass balance based approaches in [18].

REFERENCES

[1] D. Hollenbeck, D. Zulevic, and Y. Chen, "Advanced leak detection and quantification of methane emissions using suas," *Drones*, vol. 5, no. 4, p. 117, 2021.

[2] A. Shah, G. Allen, J. R. Pitt, H. Ricketts, P. I. Williams, J. Helmore, A. Finlayson, R. Robinson, K. Kabbabe, P. Hollingsworth *et al.*, "A near-field Gaussian plume inversion flux quantification method, applied to unmanned aerial vehicle sampling," *Atmosphere*, vol. 10, no. 7, p. 396, 2019.

[3] T. A. Foster-Wittig, E. D. Thoma, and J. D. Albertson, "Estimation of point source fugitive emission rates from a single sensor time series: A conditionally-sampled Gaussian plume reconstruction," *Atmospheric Environment*, vol. 115, pp. 101–109, 2015.

[4] J. R. Gemerek, S. Ferrari, and J. D. Albertson, "Fugitive gas emission rate estimation using multiple heterogeneous mobile sensors," in *2017 ISOCS/IEEE International Symposium on Olfaction and Electronic Nose (ISOEN)*. IEEE, 2017, pp. 1–3.

[5] J. D. Albertson, T. Harvey, G. Foderaro, P. Zhu, X. Zhou, S. Ferrari, M. S. Amin, M. Modrak, H. Brantley, and E. D. Thoma, "A mobile sensing approach for regional surveillance of fugitive methane emissions in oil and gas production," *Environmental science & technology*, vol. 50, no. 5, pp. 2487–2497, 2016.

[6] A. Shah, J. R. Pitt, H. Ricketts, J. B. Leen, P. I. Williams, K. Kabbabe, M. W. Gallagher, and G. Allen, "Testing the near-field gaussian plume inversion flux quantification technique using unmanned aerial vehicle sampling," *Atmospheric Measurement Techniques*, vol. 13, no. 3, pp. 1467–1484, 2020.

[7] A. Shah, H. Ricketts, J. R. Pitt, J. T. Shaw, K. Kabbabe, J. B. Leen, and G. Allen, "Unmanned aerial vehicle observations of cold venting from exploratory hydraulic fracturing in the united kingdom," *Environmental Research Communications*, vol. 2, no. 2, p. 021003, 2020.

[8] J. D'Errico, "fminsearchbnd, fminsearchcon," Feb 2022. [Online]. Available: https://www.mathworks.com/matlabcentral/fileexchange/8277-fminsearchbnd-fminsearchcon

[9] M. Krstic and H.-H. Wang, "Stability of extremum seeking feedback for general nonlinear dynamic systems," *Automatica*, vol. 36, no. 4, pp. 595–601, 2000.

[10] M. Leblanc, "Sur l'electrification des chemins de fer au moyen de courants alternatifs de frequence elevee," *Revue générale de l'électricité*, vol. 12, no. 8, pp. 275–277, 1922.

[11] S. L. Brunton, C. W. Rowley, S. R. Kulkarni, and C. Clarkson, "Maximum power point tracking for photovoltaic optimization using ripple-based extremum seeking control," *IEEE Transactions on Power Electronics*, vol. 25, no. 10, pp. 2531–2540, 2010.

[12] J. Viola, D. Hollenbeck, C. Rodriguez, and Y. Chen, "Fractional-order stochastic extremum seeking control with dithering noise for plasma impedance matching," in *Proceedings of the 2021 IEEE Conference on Control Technology and Applications (CCTA)*. IEEE, 2021, pp. 247–252.

[13] J. Cao, Y. Chen, and C. Li, "Multi-UAV-based optimal crop-dusting of anomalously diffusing infestation of crops," in *Proceedings of the 2015 American Control Conference (ACC)*. IEEE, 2015, pp. 1278–1283.

[14] Y. Chen, Z. Wang, and J. Liang, "Optimal dynamic actuator location in distributed feedback control of a diffusion process," *International Journal of Sensor Networks*, vol. 2, no. 3-4, pp. 169–178, 2007.

[15] Y. Chen, Z. Wang, and K. Moore, "Optimal spraying control of a diffusion process using mobile actuator networks with fractional potential field based dynamic obstacle avoidance," in *Proceedings of the 2006 IEEE International Conference on Networking, Sensing and Control*, 2006, pp. 107–112.

[16] Y. Chen, Z. Wang, and J. Liang, "Actuation scheduling in mobile actuator networks for spatial-temporal feedback control of a diffusion process with dynamic obstacle avoidance," in *Proceedings of the IEEE International Conference Mechatronics and Automation, 2005*, vol. 2, 2005, pp. 752–757 Vol. 2.

[17] D. Hollenbeck, D. Zulevic, and Y. Chen, "MOABS/DT: Methane Odor Abatement Simulator with Digital Twins," in *Proceedings of the 2021 IEEE 1st International Conference on Digital Twins and Parallel Intelligence (DTPI)*. IEEE, 2021, pp. 378–381.

[18] D. Hollenbeck and Y. Chen, "Characterization of ground-to-air emissions with sUAS using a digital twin framework," in *Proceedings of the 2020 International Conference on Unmanned Aircraft Systems (ICUAS)*. IEEE, 2020, pp. 1162–1166.